

A Strategy to Minimize Dust Foregrounds in B-mode Searches

Ely D. Kovetz and Marc Kamionkowski

*Department of Physics and Astronomy, Johns Hopkins University,
3400 N. Charles Street, Baltimore, Maryland 21218, USA*

(Dated: August 1, 2018)

The Planck satellite has identified several patches of sky with low polarized dust emission, obvious targets for searches for the cosmic-microwave-background (CMB) B-mode signal from inflationary gravitational waves. Still, given the Planck measurement uncertainties, the polarized dust foregrounds in these different candidate patches may differ by an order of magnitude or more. Here we show that a brief initial experiment to map these candidate patches more deeply at a single high frequency can efficiently zero in on the cleanest patch(es) and thus improve significantly the sensitivity of subsequent B-mode searches. A ground-based experiment with current detector technology operating at $\gtrsim 220$ GHz for 3 months can efficiently identify a low-dust-amplitude patch and thus improve by up to a factor 2 or 3 on the sensitivity to cosmic B modes of the subsequent lower-frequency deep integration. A balloon experiment with current detector sensitivities covering the set of patches and operating at ~ 350 GHz can reach a similar result in less than two weeks. This strategy may prove crucial in accessing the smallest gravitational-wave signals possible in large-field inflation. The high-frequency data from this exploratory experiment should also provide valuable foreground templates to subsequent experiments that integrate on any of the candidate patches explored.

PACS numbers:

A significant effort is now underway to detect the B-mode signal [1] induced by inflationary gravitational waves [2] in the polarization of the cosmic microwave background (CMB). Any such search must, however, distinguish the cosmic signal from the contamination by Galactic foregrounds, in particular polarized emission from dust, as recent experience has shown [3–6]. Recent data from the Planck satellite on polarized dust emission at 353 GHz has shown that dust polarization may be higher than had been expected, even in low-intensity regions at high Galactic latitudes [7]. The data also indicate that the amplitude of dust-intensity fluctuations in a given patch of sky is not necessarily a reliable proxy for the dust-polarization fluctuations, as had been assumed before.

The importance of the detection of inflationary B modes for cosmology motivates us to reconsider, in the light of this new information, every possible avenue to reduce the contamination from dust in CMB B-mode maps and thus maximize the sensitivity of B-mode experiments. An unambiguous detection will of course require multifrequency component separation, and a putative cosmic signal must have the correct statistical properties [8]. Still, several experiments that focus on a small (~ 400 square degrees) patch of sky [9] (e.g., BICEP3, PolarBear.....), to target the recombination peak in the B-mode power spectrum, will do better if they integrate on cleaner (i.e., lower dust-polarization foreground) patches of sky. An obvious question for these experiments is which of the ~ 100 ~ 400 -square-degree patches of the sky to survey. In the past, this selection was based on available information on dust-intensity fluctuations. Now that we have 353-GHz polarization maps

from Planck [7], the selection will be based largely upon that information.

The silver lining for B-mode searches of the Planck dust-polarization maps is the identification of a handful of patches that may potentially have much lower dust-polarization amplitudes than the average patch. The crucial point, though, is that due to the limited Planck sensitivity, the measurements in these low-dust-polarization patches are noise-dominated, and it is impossible to determine at this point which of these candidate patches is cleanest of dust-polarization foregrounds. The dust amplitudes could plausibly vary by an order of magnitude or even more.

Small-sky experiments are hence faced with a difficult choice: which of Planck’s best patches should be chosen for the deep integration required to optimize the sensitivity to B modes? Should they choose one at random and hope for the best? or perhaps split the total observation between multiple patches?

An alternative strategy, which we consider here, is to conduct a brief initial exploratory survey, at a high (dust-dominated) frequency, of the few relatively clean Planck patches to identify the cleanest of them. As we will show, a B-mode experiment that then focuses on this cleanest patch may potentially be $\sim 20\% - 66\%$ more sensitive than it would be without this initial stage of exploration. More precisely, we use as a figure of merit the lowest upper bound achievable by a null experiment on the tensor-to-scalar ratio r . We then compare the bound obtained in several different scenarios for the exploration phase to that obtained with no exploration. We show that the $\sim 20\% - 66\%$ improvement can be achieved with an initial 3-month ground-based survey at 220 GHz, with current

detector technology, or with a two-week balloon experiment at 353 GHz. We also consider briefly several strategies to optimize the initial stage of exploration. We will see that the proposed initial exploration may allow experiments to more efficiently access the lowest gravitational-wave amplitudes expected in large-field models [10, 11].

We use standard techniques (see, e.g., Ref. [12]) to estimate the sensitivity of a given experiment to B modes in the presence of foregrounds and lensing. The Fisher forecast for the error in the measurement of the amplitude A of a power spectrum C_ℓ , with some assumed multipole-moment ℓ dependence, is [9, 12],

$$\frac{1}{\sigma_A^2} = \sum_{\ell} \left(\frac{\partial C_\ell}{\partial A} \right)^2 \frac{1}{\sigma_\ell^2}. \quad (1)$$

We assume that the likelihood function is Gaussian in the vicinity of its maximum [15, 16]. To emphasize the rough nature of this approximation we use quotation marks around “ 1σ ” when referring to the error σ_A in the amplitude A .

We now consider an experiment to identify through measurements at a single high (dust-dominated) frequency ν_{dust} the cleanest of several candidate patches of sky. We assume that the observation time is divided into several steps, each dedicated to a different patch of sky. We then need to estimate the *dust amplitude* A in a targeted patch within the observation time allotted to a *single step* of the exploration stage. For a given sky coverage f_{sky} , the “ 1σ ” error to the value of A estimated from an individual multipole moment ℓ is [9, 17, 18],

$$\sigma_{\hat{A}} = \sqrt{\frac{2}{f_{\text{sky}}(2\ell+1)}} \left(\alpha C_\ell^L + f_{\text{sky}} w^{-1}(t_{\text{step}}) e^{\ell^2 \sigma_b^2} \right), \quad (2)$$

where \hat{A} denotes the estimated value of A , C_ℓ^L is the lensing B-mode contribution and $w^{-1}(t_{\text{step}})$ is the inverse weight per solid angle given an observation time t_{step} . The quantity $1 - \alpha$ parametrizes the level of de-lensing [18–20] that is applied to the data. To be conservative, we assume $\alpha = 1$ (no de-lensing) unless stated otherwise. The total “ 1σ ” error in the measurement of \hat{A} over a time t_{step} is thus,

$$\sigma_{\hat{A}} = \left[\frac{f_{\text{sky}}}{2} \sum_{\ell_{\text{min}}}^{\ell_{\text{max}}} \frac{(2\ell+1)(\tilde{C}_\ell^D)^2}{(C_\ell^L + f_{\text{sky}} w^{-1}(t_{\text{step}}) e^{\ell^2 \sigma_b^2})^2} \right]^{-\frac{1}{2}}, \quad (3)$$

where $\tilde{C}_\ell^D = C_\ell^D/A = 2\pi\ell^{-m}/[\ell(\ell+1)]$ encodes the ℓ dependence of the dust power spectrum (which we assume to be the same across the sky, as suggested by Ref. [7]) and $\ell_{\text{min}} = 40$ is the lowest multipole included in the analysis. We emphasize that we are interested in the dust amplitude A in the *particular patch* we are considering for prolonged observation, and hence no cosmic-variance term appears in Eq. (3).

After the optimal patch is identified through exploration, a prolonged stage of integration is performed over the chosen patch at a CMB-dominated frequency ν_{CMB} (and as we discuss below, perhaps additional frequencies). To estimate the gain achieved by exploration, we compare the sensitivity to primordial B modes from the integration. The smallest amplitude in a patch p detectable at “ 1σ ” (with a total observation time T spent on the chosen patch), according to Eq. (1), is then [12]

$$\sigma_p^r = \left[\frac{f_{\text{sky}}}{2} \sum_{\ell_{\text{min}}}^{\ell_{\text{max}}} \left(\frac{\sqrt{(2\ell+1)} \tilde{C}_\ell^B}{\alpha C_\ell^L + \beta A_p(\nu_{\text{CMB}}) \tilde{C}_\ell^D + f_{\text{sky}} w(T)^{-1} e^{\ell^2 \sigma_b^2}} \right)^2 \right]^{-\frac{1}{2}}. \quad (4)$$

where $A_p(\nu_{\text{CMB}})$ is the dust amplitude in the patch p (extrapolated to frequency ν_{CMB}), \tilde{C}_ℓ^B denotes the ℓ dependence of the IGW B-mode power spectrum and β is the fraction of the foreground left in the ν_{CMB} map, after component separation is performed (in a multifrequency experiment); $\beta = 1$ with only one ν_{CMB} . We set the sample variance of the primordial signal to zero in this expression (to compare with the null hypothesis).

An important issue is that of the bias stemming from dust power in cases where it is not cleaned (e.g. in a single-frequency experiment). One could attempt to resolve this in a number of ways. First, as discussed in [23], it is possible to fit simultaneously for r and A on the *integration* data, using the different ℓ -dependence of dust and gravitational waves. Another way is to employ the *exploration* measurements on the same patch of sky, either for standard component separation, or as a means of inferring the dust amplitude which could then be extrapolated to the *integration* frequencies and used to correct the data. Naturally, full component separation with multi-frequency data is the superior method, and we will assume that is possible for most of the experimental setups we consider below.

The instrumental noise in a CMB-polarization experiment is determined by the detector-array sensitivity $s = s_{\text{det}}/\sqrt{N_{\text{det}}}$ (where s_{det} is the noise-equivalent temperature NET of each detector and N_{det} is the number of detectors in the array), the angular resolution θ_{fwhm} , the sky coverage f_{sky} , and the total observation time T (which is reduced in practice by the observing efficiency). The pixel noise σ_{pix} is then determined by $\sigma_{\text{pix}} = s/\sqrt{t_{\text{pix}}}$, where $t_{\text{pix}} = T/N_{\text{pix}}$ is the observation time dedicated to each pixel. Defining the inverse weight $w^{-1}(T) = 4\pi s^2/T$ per solid angle, the angular power spectrum of the instrumental noise, assuming the experimental beam is approximately Gaussian in shape, is given by [21]

$$C_\ell^N = \frac{\Omega \sigma_{\text{pix}}^2}{N_{\text{pix}}} e^{\ell^2 \sigma_b^2} = \frac{\Omega s^2}{T} e^{\ell^2 \sigma_b^2} = f_{\text{sky}} w^{-1}(T) e^{\ell^2 \sigma_b^2}, \quad (5)$$

where $\Omega = 4\pi f_{\text{sky}}$ and $\sigma_b^2 = \theta_{\text{fwhm}}^2/(8 \ln 2)$.

In Table I we list the parameters of the instruments we consider for the exploration experiment and the subsequent B-mode integration, where for all experiments we fix the NET per detector to be $s_{\text{det}} = 480 \mu\text{K}\sqrt{\text{s}}$ (which is already surpassed by most current generation instruments). We note that these parameters are similar to those considered, e.g., in Ref. [12]. Since dust is bright at high frequencies, current-generation ground-based or balloon experiments with $N_{\text{det}} = O(10^3)$ will most likely suffice. For the prolonged integrations we also consider more sensitive experiments (see Ref. [12]), with N_{det} as high as 10^5 . We set the minimum angular resolution to $\theta_{\text{fwhm}} = 30'$ for all experiments, so that the primordial peak at $\ell \sim 80$ may be resolved. Optimistic de-lensing prospects such as we consider below will require higher resolution E-mode polarization data along with decent lensing potential estimates (e.g. via tracers such as the CIB) [13, 14]. Finally, we assume an observing efficiency of 20% and a sky coverage of $f_{\text{sky}} = 1\%$.

	Type	N_{det}	ν_{obs} [GHz]	t_{obs} [days]
Exploration1	Ground	10^3	220	90
Exploration2	Balloon	500	353	12
Integration1	Ground	10^3	150	1000
Integration2	Ground	10^4	{90, 150, 220}	1000
Integration3	Ground	10^5	{90, 150, 220}	1000

TABLE I: Table of experimental parameters for the exploration and integration experiments under consideration.

The Planck experiment reported in [7] the results of an analysis of its 353 GHz maps at high Galactic latitudes ($|b| > 35^\circ$), where 352 patches of 400 deg^2 were analyzed in the multipole range $40 < \ell < 370$, to determine the amplitude of dust polarization. This analysis identified a group of candidate patches with low dust amplitudes, although these amplitudes had large uncertainties.

In Table II, we list the amplitudes of Planck's six best candidates, normalized to the primordial gravitational-wave B-mode power spectrum at $\ell = 80$ and extrapolated down from 353 GHz to 150 GHz, assuming a modified blackbody spectrum with spectral index $\beta_d = 1.59$ and $T_d = 19.6\text{K}$, applying the unit conversion factors and color correction coefficients as explained in [22].

r_d	0.053	0.027	-0.062	-0.020	0.057	-0.031
σ_d	0.096	0.098	0.052	0.127	0.122	0.121

TABLE II: The best-fit dust amplitude r_d and its uncertainty σ_d for the six best patches identified by Planck at 353 GHz. The values shown here are normalized to the amplitude of primordial B-modes at $\ell = 80$ and extrapolated to 150 GHz assuming a modified blackbody spectrum [22].

Given the large uncertainties in the measurements of the dust amplitudes in these six patches, we cannot claim to know how much better one can do in terms of B-mode detection by locating the cleanest patch of the sky. We can, however, study the potential improvements obtained from locating the cleanest patch of sky by simulating skies consistent with Planck measurements.

To do so, we generate an ensemble of simulated skies where the dust amplitudes in the candidate set are drawn from normal distributions with the best-fit mean and variance reported by Planck $\mathcal{N}(r_d, \sigma_{r_d})$ (for each patch in each simulation, we repeat the draw until a positive amplitude is drawn), and calculate ensemble averages for all desired quantities. We then use the conversion convention described above to transform between 150 GHz and either 220 GHz or 353 GHz.

In Table III, we calculate the lowest detectable tensor-to-scalar ratio for the worst, mean, and best foreground amplitude, averaged over the ensemble of simulations, assuming a single-frequency experiment (where $\beta = 1$) as well as multifrequency experiments, where after component separation a residual of either $\beta = 10\%$ or $\beta = 1\%$ is left, with and without de-lensing (we consider either no de-lensing, $\alpha = 1$, or an optimistic 90% de-lensing, $\alpha = 0.1$). The parameters for these B-mode-integration experiments are taken from Table I.

We should mention that there is some redundancy in the scenarios covered in Tables I and III. With no de-lensing, for example, the third integration experiment will be lensing-noise limited in a small patch of sky and will not exceed the sensitivity of the second experiment, unless a larger area of sky is covered, to reduce the sample-variance error. For simplicity, we neglect such optimizations here as our main concern is the effect of foreground reduction (by means of avoidance) and our figure-of-merit is the lowest bound achievable on the tensor-to-scalar ratio under the null hypothesis. Naturally, these considerations should play a dominant role when planning an actual experimental strategy for a given instrument (along with various other considerations, e.g. constraints on the observing efficiency in different regions of the sky).

Clearly, there is room for improvement if cleaner patches can be identified before the prolonged integration is done. We therefore turn to investigate how best to identify the cleanest patch.

Given a set of candidate patches for which we have rough dust-amplitude estimates, we can choose to forgo exploration (and just choose the best candidate according to the available data, uncertain as it may be) or to pursue a uniform exploration of all patches so as to lower the measurement uncertainty in the dust amplitude and

	β	Worst	Mean	Best	Worst $\alpha = 0.1$	Mean $\alpha = 0.1$	Best $\alpha = 0.1$
Integration1	1	0.034	0.022	0.011	0.03	0.018	0.009
Integration2	1	0.025	0.014	0.006	0.019	0.01	0.003
Integration2	10%	0.007	0.005	0.004	0.0033	0.0022	0.0011
Integration3	1	0.023	0.013	0.005	0.016	0.008	0.002
Integration3	10%	0.006	0.005	0.003	0.0024	0.0014	0.0006
Integration3	1%	0.0033	0.0031	0.0029	0.0007	0.0005	0.0004

TABLE III: Table of expected lower bounds on r with different integrations, with no exploration.

thus allow a more substantiated choice. Alternatively, one could adopt an adaptive strategy, whereby the allocation of exploration time is determined on-the-fly according to the gathered results. In this case, patches that acquired data indicate are most likely inferior are discarded early on, leaving more time to explore more deeply the remaining patches and thus zero in efficiently on the best ones.

In Ref. [23], we investigated a variety of adaptive-survey strategies for ground-based single-frequency experiments (similar to BICEP2). We showed how to construct adaptive survey strategies, based on machine-learning algorithms, to maximize the sensitivity to primordial B-modes by spending more time observing lower-foreground patches. We concluded that a wisely chosen adaptive-survey strategy could improve the upper limit to B modes (assuming a null experiment) by a factor of 2–3.

Here, though, we consider a limited fixed-time exploration at a dust-dominated high frequency which is then followed by a prolonged integration at CMB frequencies. In this case, the advantage of adaptive strategies is limited, first because the measurements are easier and secondly because there is no price paid in terms of integration time (the integration is done separately, by an independent CMB-frequency measurement). Nevertheless, we compare the performance of the adaptive Upper Confidence Bound (UCB) adaptive-survey algorithm (which was found in Ref. [23] to be quite effective) to a more naive uniform exploration to study the improvements that can be made if a given experiment can move quickly between patches at low cost.

In Fig. 1, we track the average 1σ bound on the tensor-to-scalar ratio r that may be reached by a subsequent integration experiment (we plot the results for the instrument *Integration2* with $\beta = 10\%$ and $\alpha = 0.1$), given each additional day of exploration. At each point in time, we plot the achievable bound on the tensor-to-scalar ratio r assuming it observes the patch with the lowest-measured dust amplitude by the exploration experiment up to that stage. In the top panel we show results from a ground-based experiment and in the bottom from a balloon instrument, with parameters from Table I. As

explained above, we compare three strategies. The black solid line shows the average daily bound assuming a patch is chosen at random and no exploration performed (hence no improvement). Its range of performance is shown in grey. The red solid line shows the daily bound as the patches are consecutively observed, each for a period of 15 days in the case of the ground-based instrument (or two days for the balloon). During the first observation period, there would be no gain compared to choosing at random, as expected. Then, as each additional patch is observed, the projected bound on r improves as more information is gathered to allow an intelligent choice of patch for integration. The range of performance of this method is shown in red. Finally, the blue solid line shows the daily bound with the UCB method, which converges onto cleaner patches much more quickly, but requires a flexible experiment which can switch between patches every three days (or a single day, for the balloon experiment). As can be seen, the worst case when adopting this strategy is almost always better than with the other methods.

How well will the B-mode searches (the integrations) perform if they are preceded by a stage of exploration as described above? In Table IV we present the average and worst-case B-mode limits achievable by the same integration experiments considered in Table III, after the ground-based exploration experiment in Table I has been performed to identify the optimal patch for observation in each simulation. (The balloon-borne exploration yields very similar results, so we do not show them separately). We see that the improvement compared to the *mean* without exploration ranges from 20% to 66% in almost all experiments, depending on the level of foreground subtraction and the amount of de-lensing. Another advantage of the exploration stage is that the worst case is now greatly reduced compared to the non-exploration case, as can be seen clearly.

The only case in which there is only minor improvement, $< 5\%$, is with $N_{\text{det}} = 10^5$, 1% foreground residuals, and no de-lensing. There is no improvement here as both the foreground residuals and instrumental noise are lower than the lensing B modes for all six patches and hence there is no gain by focusing on cleaner ones. Such a tactic, though, cannot reach the value $r \simeq 0.002$ that is targeted to fully probe the parameter space for large-field-inflation.

To conclude, we have considered the benefits for B-mode searches of an initial exploratory experiment to measure at a single high (dust-dominated) frequency the dust-polarization amplitudes in several candidate low-dust-polarization patches identified by Planck. We have shown that the sensitivity of the subsequent B-mode searches can be improved, with the identification of the

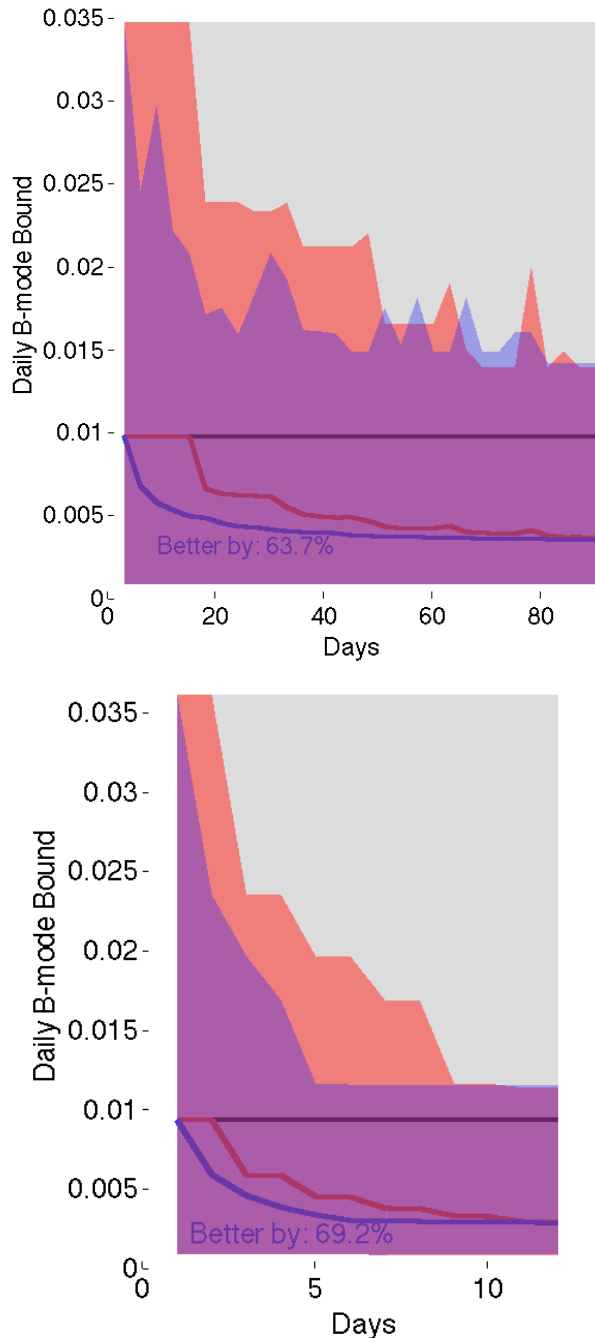


FIG. 1: The projected “ 1σ ” bound on the tensor-to-scalar ratio r with the instrument *Integration2* with $\beta = 10\%$ and $\alpha = 0.1$ (see Table I), achievable with the information obtained from x days of exploration. We plot the results given a ground-based experiment (*Top*), or a balloon-borne one (*Bottom*), both with parameters taken from Table I. Three methods are compared: no exploration (solid black line); consecutive equal-time observation (solid red line); an adaptive method (UCB) (solid blue line). The ranges of performance are also shown (in corresponding color shades) to demonstrate the worst case for each method. After all patches are observed for $1/6$ th of the total exploration time, the uniform method reaches the same bound as the adaptive one.

	β	Worst	Mean ($\Delta(\%)$)	Worst $\alpha = 0.1$	Mean $\alpha = 0.1$	$\Delta(\%)$
Integration1	1	0.025	0.012 (39%)	0.0213	0.0098 (45%)	
Integration2	1	0.019	0.007 (51%)	0.0142	0.0036 (64%)	
Integration2	10%	0.006	0.004 (21%)	0.0028	0.0013 (39%)	
Integration3	1	0.015	0.006 (53%)	0.0099	0.0027 (66%)	
Integration3	10%	0.005	0.003 (23%)	0.0018	0.0007 (50%)	
Integration3	1%	0.003	0.003 (<5%)	0.0007	0.0004 (20%)	

TABLE IV: Table of expected lower bounds on r with different integration experiments, following a stage of exploration. Results are shown for three integration experiments with parameters listed in Table I, assuming different levels of foreground residuals (from 100% to 1%) and of de-lensing ($\alpha = 1$ for no-de-lensing or $\alpha = 0.1$ for 90% de-lensing). The improvement achievable on average compared to the non-exploration case is shown in parentheses.

cleanest patch with such an exploration, so that the upper bound achievable on the tensor-to-scalar can be decreased by as much as $\sim 20\% - 66\%$ (or as much as a factor of 3 lower). We showed that adaptive-survey strategies for the exploration experiment can allow the cleanest patch to be identified a bit more efficiently if the experiment has the flexibility to rapidly change targets. However, the improvement over a simpler rigid exploration is not particularly significant.

Although we have assumed in the analysis just one deep integration experiment, there are likely to be a significant number of independent projects, over the coming years, seeking inflationary B modes. The single exploration experiment to identify the cleanest patch is therefore likely to benefit all subsequent experiments, allowing each of them $\sim 20-66\%$ improvements in sensitivity. The deep data from the exploratory experiment (particularly one at 353 GHz) should also provide valuable foreground templates for subsequent CMB experiments on *any* of the candidate patches explored. Finally, such data may also be useful to improve our theoretical understanding of dust-polarization by clarifying some of the open questions and issues raised by Planck [7].

All of this improvement comes at the expense of just 90 days of observation from the ground at 220 GHz or two weeks by a balloon operating at 353 GHz. This price seems affordable.

We thank the anonymous referee for important comments which helped improve the clarity of our paper. This work was supported by the John Templeton Foundation, the Simons Foundation, NSF grant PHY-1214000, and NASA ATP grant NNX15AB18G.

[1] M. Kamionkowski, A. Kosowsky and A. Stebbins, Phys. Rev. Lett. **78**, 2058 (1997) [arXiv:astro-ph/9609132];

- U. Seljak and M. Zaldarriaga, Phys. Rev. Lett. **78**, 2054 (1997) [arXiv:astro-ph/9609169]; M. Kamionkowski, A. Kosowsky and A. Stebbins, Phys. Rev. D **55**, 7368 (1997) [astro-ph/9611125]; M. Zaldarriaga and U. Seljak, Phys. Rev. D **55**, 1830 (1997) [astro-ph/9609170].
- [2] L. F. Abbott and M. B. Wise, Nucl. Phys. B **244**, 541 (1984); V. A. Rubakov, M. V. Sazhin and A. V. Veryaskin, Phys. Lett. B **115**, 189 (1982); R. Fabbrì and M. d. Pollock, Phys. Lett. B **125**, 445 (1983); A. A. Starobinsky, JETP Lett. **30**, 682 (1979) [Pisma Zh. Eksp. Teor. Fiz. **30**, 719 (1979)].
- [3] P. A. R. Ade *et al.* [BICEP2 Collaboration], Phys. Rev. Lett. **112**, 241101 (2014) [arXiv:1403.3985 [astro-ph]].
- [4] R. Flauger, J. C. Hill and D. N. Spergel, JCAP **1408**, 039 (2014) [arXiv:1405.7351 [astro-ph]].
- [5] M. J. Mortonson and U. Seljak, [arXiv:1405.5857].
- [6] P. A. R. Ade *et al.* [BICEP2 and Planck Collaborations], http://new.bicepkeck.org/BKP_paper_20150130.pdf
- [7] R. Adam *et al.* [Planck Collaboration], arXiv:1409.5738 [astro-ph.CO].
- [8] M. Kamionkowski and E. D. Kovetz, Phys. Rev. Lett. **113**, no. 19, 191303 (2014) [arXiv:1408.4125 [astro-ph]].
- [9] A. H. Jaffe, M. Kamionkowski and L. -M. Wang, Phys. Rev. D **61**, 083501 (2000) [astro-ph/9909281].
- [10] D. H. Lyth, Phys. Rev. Lett. **78**, 1861 (1997) [hep-ph/9606387].
- [11] G. Efstathiou and K. J. Mack, JCAP **0505**, 008 (2005) [astro-ph/0503360].
- [12] W. L. K. Wu, J. Errard, C. Dvorkin, C. L. Kuo, A. T. Lee, P. McDonald, A. Slosar and O. Zahn, arXiv:1402.4108 [astro-ph.CO].
- [13] K. M. Smith, D. Hanson, M. LoVerde, C. M. Hirata and O. Zahn, JCAP **1206**, 014 (2012) [arXiv:1010.0048 [astro-ph.CO]].
- [14] B. D. Sherwin and M. Schmittfull, arXiv:1502.05356 [astro-ph.CO].
- [15] G. Jungman, M. Kamionkowski, A. Kosowsky and D. N. Spergel, Phys. Rev. D **54**, 1332 (1996) [astro-ph/9512139].
- [16] W. Zhao, D. Baskaran and L. P. Grishchuk, Phys. Rev. D **79**, 023002 (2009) [arXiv:0810.0756 [astro-ph]].
- [17] L. Knox and Y. -S. Song, Phys. Rev. Lett. **89**, 011303 (2002) [astro-ph/0202286].
- [18] M. Kesden, A. Cooray and M. Kamionkowski, Phys. Rev. Lett. **89**, 011304 (2002) [astro-ph/0202434].
- [19] K. Sigurdson and A. Cooray, Phys. Rev. Lett. **95**, 211303 (2005) [astro-ph/0502549].
- [20] K. M. Smith, D. Hanson, M. LoVerde, C. M. Hirata and O. Zahn, JCAP **1206**, 014 (2012) [arXiv:1010.0048].
- [21] M. Tegmark, Phys. Rev. D **56**, 4514 (1997) [astro-ph/9705188].
- [22] P. A. R. Ade *et al.* [Planck Collaboration], A. & A. , **571**, 27 (2014), arXiv:1303.5070 [astro-ph.IM].
- [23] E. D. Kovetz and M. Kamionkowski, arXiv:1308.1404 [astro-ph.IM].